



## ISTITUTO NAZIONALE DI RICERCA METROLOGICA Repository Istituzionale

### Memristive Devices for Quantum Metrology

This is the author's submitted version of the contribution published as:

*Original*

Memristive Devices for Quantum Metrology / Milano, Gianluca; FERRARESE LUPI, Federico; Fretto, Matteo; Ricciardi, Carlo; DE LEO, Maria; Boarino, Luca. - In: ADVANCED QUANTUM TECHNOLOGIES. - ISSN 2511-9044. - 3:5(2020), p. 2000009. [10.1002/qute.202000009]

*Availability:*

This version is available at: 11696/64796 since: 2021-01-29T12:08:13Z

*Publisher:*

WILEY

*Published*

DOI:10.1002/qute.202000009

*Terms of use:*

This article is made available under terms and conditions as specified in the corresponding bibliographic description in the repository

*Publisher copyright*

WILEY

This article may be used for non-commercial purposes in accordance with Wiley Terms and Conditions for Use of Self-Archived Versions

(Article begins on next page)

## Memristive devices for quantum metrology

*Gianluca Milano<sup>1,2\*</sup>, Federico Ferrarese Lupi<sup>1</sup>, Matteo Fretto<sup>1</sup>, Carlo Ricciardi<sup>2</sup>, Natascia De Leo<sup>1</sup>, Luca Boarino<sup>1</sup>*

<sup>1</sup>Advanced Materials Metrology and Life Science Division, INRiM (Istituto Nazionale di Ricerca Metrologica), Strada delle Cacce 91, 10135 Torino, Italy.

<sup>2</sup>Department of Applied Science and Technology, Politecnico di Torino, C.so Duca degli Abruzzi 24, 10129 Torino, Italy.

E-mail: g.milano@inrim.it

Keywords: metrology, quantized conductance, quantum point contact, memristive devices, resistive switching

As a consequence of the redefinition of the International System of Units (SI) where units are defined in terms of fundamental physical constants, memristive devices represent a promising platform for quantum metrology. Coupling ionics with electronics, memristive devices can exhibit conductance levels quantized in multiples of the fundamental quantum of conductance  $G_0=2e^2/h$ . Since the fundamental quantum of conductance  $G_0$  is related only on physical constants that assume a fixed value in the revised SI, memristive devices can be exploited for the practical realization of a quantum-based resistance standard. Differently from quantum-Hall effect devices conventionally adopted for the realization of a resistance standard whose working principles requires cryogenic temperatures and/or high magnetic fields, memristive devices can operate in air at room temperature without the need of an applied magnetic field. In memristive devices, quantized conductance effects are related to ionic processes at the nanoscale that regulate the resistive switching mechanism underlying memristive behaviour. Thanks to the high operational speed, high scalability down to the nanometer scale and CMOS compatibility, memristive devices allows on-chip implementation of a resistance standard required for the

realization of self-calibrating electrical systems and equipment with zero-chain traceability in accordance with the new SI.

## **Introduction**

The year 2019 represents an historic revolution for metrology as the science of measurement because of the redefinition of the International System of Units (SI), as ratified by the General Conference on Weights and Measures (Conférence générale des poids et mesures, CGPM).<sup>[1,2]</sup> The revised SI represents an important change of paradigm for metrology: all SI units are now defined in terms of fundamental constants of Nature. This means that the seven base units (second, meter, kilogram, ampere, kelvin, mole and candela) are defined in terms of seven defining constants (the hyperfine transition frequency of the caesium 133 atom, the speed of light in vacuum, the Planck constant, the elementary charge, the Boltzmann constant, the Avogadro constant and the luminous efficacy of a defined visible radiation) that are assigned to an exact numerical value. Because of the fixed exact value without uncertainty, these fundamental constants in the revised SI have not to be measured anymore. As a direct consequence, each experiment that is able to correlate a measurable quantity to a fundamental constant of Nature (or a combination of fundamental constants) becomes a direct realization of the corresponding SI unit. This redefinition opens the way for the development of new experiments and devices where the uncertainty in the realization of the units depends on the specific technical/scientific purpose. In this framework, there is a growing interest in the realization of experiments and devices that allows integration of fundamental units as internal standard references for the realization of self-calibrating embedded systems with zero-chain traceability. This is particularly true for electrical systems where the on-chip integration of electrical units can pave the way for the realization of self-calibrating electronic devices and measurements equipment. The practical realization of electrical units is conventionally achieved by means of devices exploiting quantum effects such as the quantum Hall effect, the Josephson effect and the single electron transistor effect.<sup>[3–5]</sup> However, these effects are

observed in vacuum conditions at cryogenic temperatures and/or in presence of high magnetic fields usually obtainable only in a laboratory environment. All these requirements strictly hamper the scalability and on-chip integration of these metrological devices.

In this work we propose the realization of a standard of resistance by means of a simple two-terminal memristive device that exhibits well defined quantized resistance states depending on the input electrical stimuli. These quantum conductance effects can be observed in air at room temperature. Despite at the cost of a larger uncertainty compared to quantum Hall based resistance standards, memristive devices are here proposed as a promising platform towards the on-chip implementation of a resistance standard due to the high scalability down to the nanometer size and the compatibility with the conventional CMOS technology. This can allow the realization of electrical systems and measurement equipment with embedded self-calibrating systems that have traceability to fundamental physical quantities in accordance to the new SI.

## Discussion

In electrical metrology, the new SI implies that electrical quantities such as voltage, current and resistance are redefined by fixing the value of the fundamental charge  $e$  and the Planck constant  $h$  (Figure 1a). This implies that it is possible to define electrical units abrogating the conventional definition of Josephson and von Klitzing constants  $K_{J-90}$  and  $R_{K-90}$  that were conventionally assigned to fixed values in 1990 ( $K_{J-90} = 483\,597.9$  GHz/V,  $R_{K-90} = 25812,807$   $\Omega$ ) to allow a more precise realization of electrical units respect to the theoretical (electromechanical) definition of the Ampere.<sup>[6]</sup> Josephson and von Klitzing constants are now fixed in terms of  $e$  and  $h$  according to the relationships  $K_J = 2e/h$  ( $K_J = 2e/h = 483\,597.848\,416\,984 \dots$  GHz/V) and  $R_K = h/e^2$  ( $R_K = 25\,812.807\,459\,304\,5\dots$   $\Omega$ ), embedding the realization of volt and ohm in the new SI. Independently from the redefinition of the SI, quantum experiments represent the most accurate approach for the *mise en pratique* of electrical units. While

quantized effects in Josephson junctions and Coulomb blockade in single electron transistors are adopted for the realization of the standard representation of voltage and current, respectively, quantum Hall effects are exploited for the realization of the standard of resistance.<sup>[4]</sup>

The quantum-mechanical version of the Hall effect can be observed in two-dimensional electron systems in presence of low temperatures and strong magnetic fields where the Hall conductance exhibits quantized values (Hall plateaus) multiples of  $e^2/h$ , thus enabling the definition of the electrical resistance in terms of the von Klitzing constant  $R_K$ .<sup>[7,8]</sup> This effect was investigated in devices based on heterostructures of semiconductor materials such as silicon or gallium arsenide in contact with an insulator material (such as SiO<sub>2</sub> or AlGaAs).<sup>[8]</sup> The observation of quantized conductance plateaus was firstly reported by Von Klitzing et al. at temperatures and magnetic fields of 4.2 K and 15 Tesla, respectively.<sup>[7]</sup> Although recent developments show that quantized Hall effects can be observed also at room temperature in 2D materials such as graphene,<sup>[9]</sup> devices for observing quantized Hall effect necessarily requires multiterminal electrical measurements in presence of a magnetic field in order to measure the transversal resistance when electronic current is injected in the longitudinal direction, as schematized in Figure 1b. In this scenario, memristive devices coupling ionics with electronics can offer a promising platform to observe quantum effects that can be traced to fundamental physics constants. As discussed in the following, these effects can be observed in two terminal memristive devices (Figure 1c) working in air at room temperature.

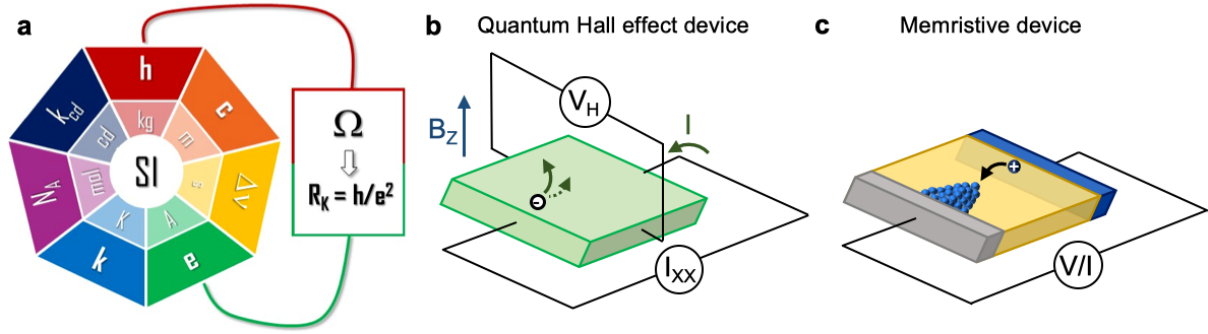


**Figure 1.** The new SI and the standard of resistance. **a** Units and defining constants in the new SI. The standard of resistance is defined by fixing the values of the fundamental charge  $e$  and the Planck constant  $h$ , through the von Klitzing constant  $R_K$ . Device configuration for **b** quantum Hall effect involving multiterminal measurements and **c** two-terminal memristive device for observing quantized conductance effects required for the realization of a standard of resistance.

Memristive devices relying on redox-based resistive switching phenomena are two terminal devices where the internal state of resistance depends on the history of applied voltage/current. [10–12] The change of the internal state of resistance under external electrical stimulation of the device, that usually consists of a simple metal/insulator/metal sandwich structure, is related to atomic reconfiguration phenomena involving nanoionic processes.<sup>[11]</sup> In case of electrochemical metallization memory (ECM) cells, an applied voltage to an electrochemically active electrode (usually Ag or Cu) is responsible for redox reactions involving dissolution of metal atoms to form metal ions that migrate in the insulating matrix under the action of the applied electric field.<sup>[13]</sup> Subsequent reduction and electro-crystallization of ions leads to the formation of a metallic conductive path (filament) bridging the two electrodes that is responsible for an increased device conductivity. A schematization of the resistive switching mechanism is reported in Fig. 2a. The formation/rupture of this metallic filament under external electrical stimuli leads to the resistive switching behaviour responsible for the change of resistance in between a low resistance state (LRS) and a high resistance state (HRS). Similarly, resistive switching behaviour can be observed in valence change memory (VCM) cells, where ionic species involved in the formation/rupture of the conductive path are oxygen-related

defects such as oxygen vacancies.<sup>[11]</sup> In both ECM and VCM configuration an initial step termed electroforming process is usually required to initialize the conductive path before observing SET/RESET processes.<sup>[14]</sup> It is worth noticing that the above described resistive switching phenomena are observed in a wide range of materials such as metal-oxide thin films and nanostructures, perovskites and organic materials.<sup>[15–17]</sup>

Interestingly, if the size of the conductive filament is reduced to the atomic scale, memristive devices exhibits quantized effects of conductivity typical of ballistic electron transport through a constriction (quantum point contact).<sup>[18,19]</sup> In such systems, quantum size effects are expected to become relevant when the filament size is in the order of the phase coherence length of the electrons. In this case, the atomic-sized conductive path behaves as an electron waveguide where conduction does not follow the Ohm's law.<sup>[20,21]</sup> While metal electrodes act as electron reservoirs, the conductive filament bridging the two electrodes results in a ballistic electron conduction path constituted by discrete conductive channels. Each of these conduction channels contributes with a maximum amount of one fundamental quantum of conductance  $G_0 = 2e^2/h$  to the total conductance. Based on the Landauer approach, a quantum point contact (QPC) model describing such quantization of conductance in memristive devices was proposed by Miranda et al..<sup>[22]</sup> In the QPC model, quantum transport through a 3D tube-like constriction can be described by means of a 1D tunneling behavior. In this case, the energy dispersion curve of electrons consists of discrete parabolic sub-bands, where the spacing in between sub-bands depends on the filament morphology. In this framework, the electronic current flowing through the quantum point contact under application of an external bias  $V$  is given by the expression:<sup>[18,19]</sup>

$$I(V) = \frac{2e}{h} N \int_{-\infty}^{\infty} T(E) [f(E - \beta eV) - f(E + (1 - \beta)eV)] dE \quad (1)$$

where  $N$  (integer number), is the number of the 1D conductive channels contributing to the conduction,  $T$  is the transmission probability,  $E$  is the energy,  $f$  is the Fermi distribution,  $e$  the

electron charge,  $h$  is the Planck constant and  $\beta$  is the asymmetry parameter representing the fraction of the applied bias that drops on the source side of the constriction ( $0 \leq \beta \leq 1$ ). Considering the expression for  $T$  derived from the assumption of an inverted parabolic potential barrier for the quantized sub-bands into the constriction:<sup>[18,19,23]</sup>

$$T(E) = \{1 + \exp[-\alpha(E - \varphi)]\}^{-1} \quad (2)$$

where  $\alpha$  is a constant related to the potential barrier curvature of the sub-bands and  $\varphi$  is the barrier height, by inserting eq. (2) in eq. (1), the expression for  $I$  can be rewritten as:<sup>[18,19,23]</sup>

$$I(V) = \frac{2e}{h} N \left\{ eV + \frac{1}{\alpha} \ln \left[ \frac{1 + \exp\{\alpha[\varphi - \beta eV]\}}{1 + \exp\{\alpha[\varphi + (1 - \beta)eV]\}} \right] \right\} \quad (3)$$

Note that eq. (3) can describe both HRS and LRS of a memristive device by properly adjusting the values of  $\alpha$  and  $\varphi$ . In the HRS, where conductive filament is not continuous, for low applied voltages eq. (3) converges to:<sup>[18]</sup>

$$I(V) = N G_0 \exp(-\alpha \varphi) V \quad (4)$$

In this case, the electronic conduction is regulated by the barrier that is described by  $\alpha$  and  $\varphi$  parameters. In the LRS, where the metallic conductive filament is continuous, eq. (3) converges to:<sup>[18]</sup>

$$I(V) = N \beta G_0 V \quad (5)$$

Thus, the conductance shows integer multiples of the fundamental quantum of conductance  $G_0$  when the voltage drop across the two interfaces is asymmetric ( $\beta=1$ ), according to the relationship:

$$G = N G_0 \quad (6)$$

In this case, it turns out that the quantized conductance values depend only on constant of Nature fixed to an exact value in the new SI and are related to the von Klitzing constant through the relation  $G_0 = 2/R_K$ . Since the Fermi wavelength in a metal is of the same order of magnitude of atomic separation,<sup>[20]</sup> a quantum point contact in memristive devices requires atomic dimensions of the filament where the number of activated conductive channels ( $N$ ) depends on



its size and geometry. As schematized in figure 2b, the memristive cell exhibit  $G \ll G_0$  when the device is in the HRS and electronic conduction can occur through tunneling effects across the filament gap,  $G \sim G_0$  when the filament size is close to the atomic scale while  $G \gg G_0$  by increasing the filament size to few nanometers where conduction occurs according to the Ohm's law and quantum effects are suppressed. An important aspect is that quantum conductance effects can be observed at room temperature since the quantum mode splitting is typically in the order of about 1 eV.<sup>[21]</sup>

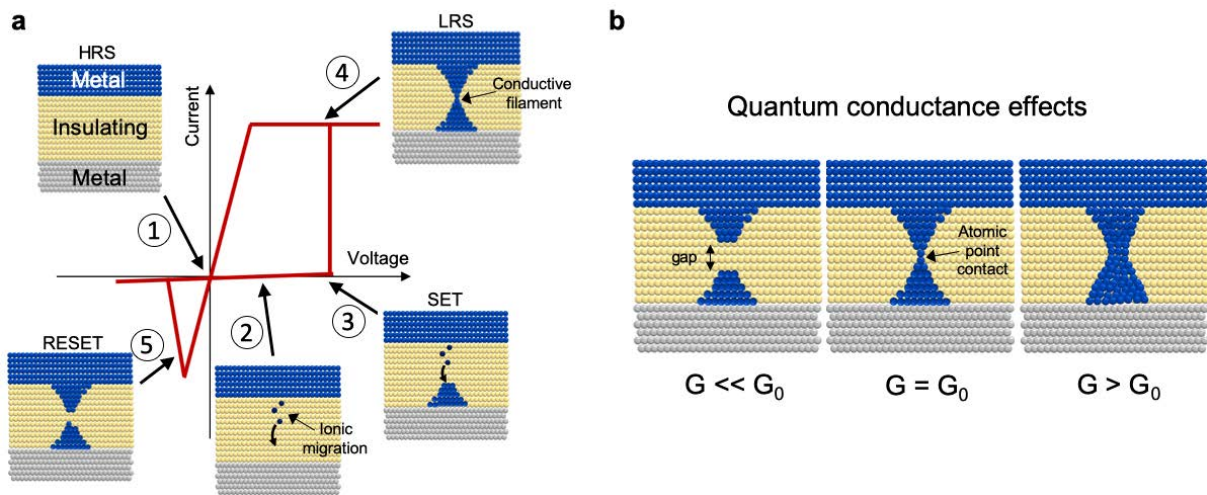


**Figure 2.** Resistive switching phenomena and quantum conductance effects in memristive devices. **a** Working principle of a memristive device involving nanoionics processes with formation/rupture of a conductive path (filament) across the insulating layer that is responsible for resistive switching behaviour from an high resistance state (HRS) to a low resistance state (LRS) and viceversa. **b** Quantum conductance effects can be observed when the filament is scaled down to the atomic scale. Electronic conduction occurs through tunneling with  $G \ll G_0$  when the filament is not continuous (HRS state), filament with atomic size results in  $G \sim G_0$  while  $G \gg G_0$  when the filament size is increased to few nanometers.

Despite the observation of quantized conductance values in resistive switching devices already in the '90s,<sup>[24,25]</sup> the interest on memristive devices exhibiting quantized conductance becomes relevant after that Terabe et al.<sup>[26]</sup> reported in 2005 high control of quantized conductance values in two-terminal atomic switch memristive devices. In this work, well defined quantized conductance levels were obtained by electrochemically controlling the growth/rupture of a silver protusion in a silver-sulphide ( $\text{Ag}_2\text{S}$ ) matrix through external electrical stimulation. After

this seminal work, experimental evidences of conductance quantization were reported in a wide range of memristive cells based on different material systems both in ECM and VCM configuration.<sup>[27,28,37–39,29–36]</sup> Independently from the memristive mechanism, the observation of quantum effects requires an accurate control of the filament size and morphology at the atomic level by means of appropriate external electrical stimulations of the device. In this context, quantized conductance effects have been reported by means of a wide range of operating methods employed to probe the memristive device response to external electrical stimulations. The most common method of stimulation is the voltage sweep mode where a voltage ramp is applied to the device. Under this stimulation, quantized steps of conductance were reported during both SET and RESET operations as a consequence of the progressive formation and rupture of the filament, respectively<sup>[18,27,42,30,31,33,35,37,39–41]</sup> An example of quantization phenomena observed during the RESET process in Pt/HfO<sub>2</sub>/Pt memristive devices by Li et al.<sup>[18]</sup> is reported in Fig. 3a. As can be observed, a voltage sweep applied to the device resulted in a gradual RESET process with an increasing of device resistance in a quantized manner due to the progressive rearrangement of atoms during the final stage of filament dissolution. During voltage sweeps, the filament morphology responsible for quantized resistance levels can be also modulated by controlling the maximum current flowing into the device and/or by the applied voltage range.<sup>[35]</sup> Current sweep operation mode was reported by Tappertzhofen et al.<sup>[36]</sup> to be responsible for the observation of more discrete resistance levels compared to the voltage sweep operation mode in AgI memristive cells. Quantized steps of conductance can be observed also in constant voltage bias operation mode.<sup>[27,28,34,40]</sup> Indeed, when an appropriate bias voltage is applied to the cell, a stepwise increasing/decreasing of conductivity with multiples of  $G_0$  can be observed over a large time scale. For example, this effect was reported by Tsuruoka et al.<sup>[28]</sup> in Ag/Ta<sub>2</sub>O<sub>5</sub>/Pt memristive cells where quantized conductance steps are observed in the current time trace under the application of a small constant bias. As an alternative, the internal resistance state can be changed at steps of quantum conductance under device stimulation by

means of voltage pulses.<sup>[28–30,41]</sup> By properly adjusting pulse parameters such as amplitude, width and time interval between pulses, quantized conductance levels can be observed in both SET and RESET processes as reported in Figure 3d and e. It is worth noticing that the modulation of the quantized conductance levels was demonstrated by device stimulation with pulses down to the nanosecond timescale,<sup>[29]</sup> making memristive devices particularly promising for the realization of high-speed metrological devices.

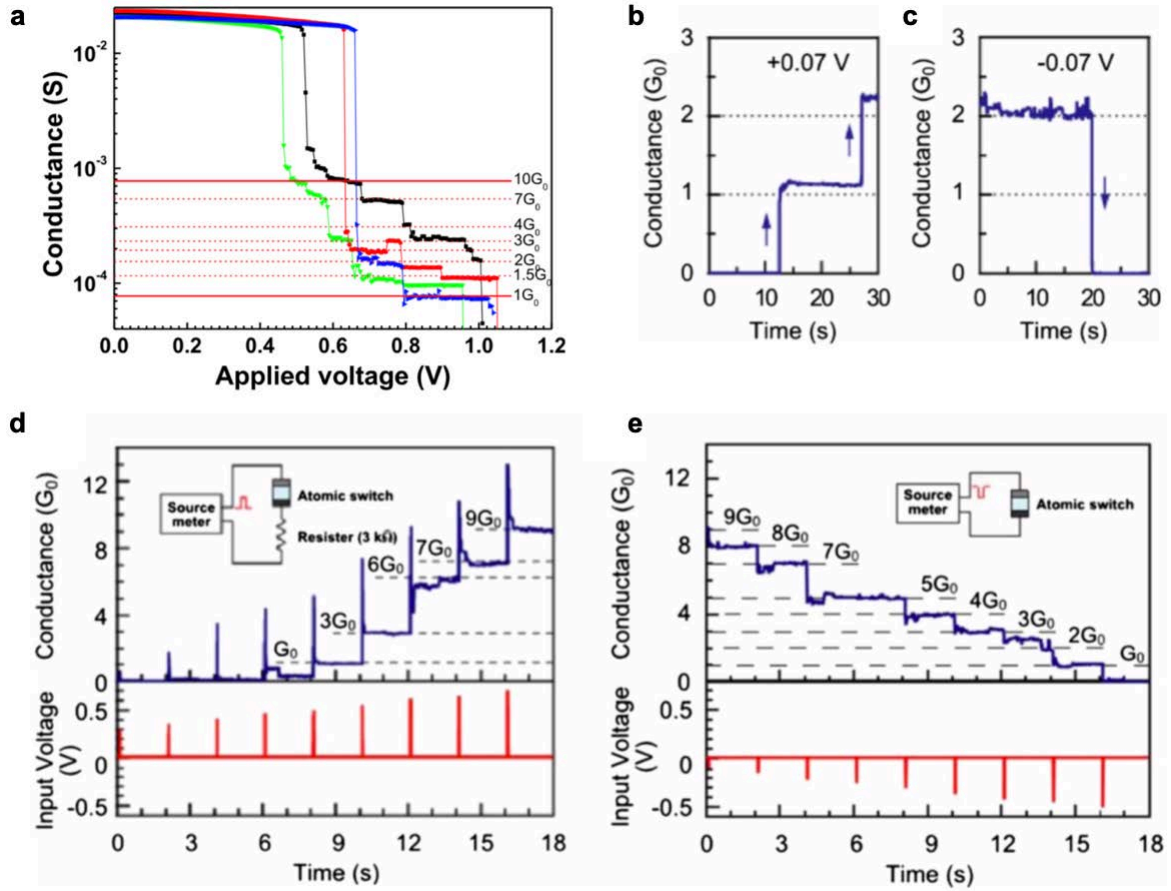


**Figure 3.** Quantum conductance effects in memristive devices. **a** Quantization phenomena observed in Pt/HfO<sub>2</sub>/Pt memristive devices during the RESET process in voltage sweep operation mode. Reproduced under the terms of Creative Commons Attribution 4.0 License.<sup>[18]</sup> Copyright 2015, Springer. Stepwise change of conductance in Ag/Ta<sub>2</sub>O<sub>5</sub>/Pt memristive devices in constant voltage bias operation mode during **b** SET and **c** RESET processes; modulation of the internal state of the memristive device in voltage pulse operational mode during **d** SET and **e** RESET process. During SET (panel d), a resistor was inserted in series to the memristive device in order to limit the maximum allowed current. Reproduced with permission.<sup>[28]</sup> Copyright 2012, IOP Publishing.

Independently from the operational mode, these experimental results show conductance quantization effects in memristive devices as a consequence of the filament evolution in terms of single atomic point contact units. In this framework, it is clear that the main challenge for the realization of metrological devices is represented by the control of the filament evolution that requires a deep understanding of the kinetics of nanoionics effects underlaying resistive switching phenomena. It is worth noticing that the control of the filament evolution and morphology necessarily implies a proper selection of the involved materials. In case of electrodes, the choice of the metal material has to be related to its electrochemical properties, i.e. its tendency toward dissolution to form ions. Instead, the choice of the active insulating material has to be related not only to its chemical properties but also to its structural properties (i.e. amorphous or crystalline phase, presence of grain boundaries etc.), density and porosity. Indeed, all these aspects strongly impact the electrochemistry of the cell and ionic transport properties. In this framework, proper design rules that relates material properties and operational conditions to the observation of quantized conductance effects are still missing. One of the main challenges related to the development of a memristive device as a standard of resistance is the intrinsic stochasticity of atomic rearrangement during the formation/rupture of the conductive filament that strongly affect reproducibility. In order to face stochasticity, that is responsible for fluctuations of conductance values, a statistical approach to acquire and analyse experimental data can be adopted. By means of a statistical analysis, the histogram of conductance values can evidence the occurrence of peaks at integer multiples of  $G_0$ , as for example reported in Figure 4a. An important observation is that, in some memristive device configurations, the conductance can be quantized also in half-integer multiples of  $G_0$ .<sup>[27,37]</sup> As an example, the latter case can be observed in the histogram of conductance changes during conductance steps in  $\text{SiO}_x$ -based memristive devices (Figure 4b). Despite this aspect still needs further investigation, the origin of this half-integer quantization has been attributed to large chemical potential differences in between the two electron reservoir metallic contacts<sup>[37]</sup> or to

the absence of spin degeneracy<sup>[18]</sup>. Another important challenge is represented by the stability over time of the internal resistance state. Indeed, conductive filaments in memristive devices can spontaneously dissolve over time without the need of an external electrical stimulation. The driving process of filament dissolution is the nanobattery effect including the Gibbs-Thomson effect of minimization of interfacial energy and electromotive forces occurring in the electrochemical memristive cell.<sup>[43–45]</sup>

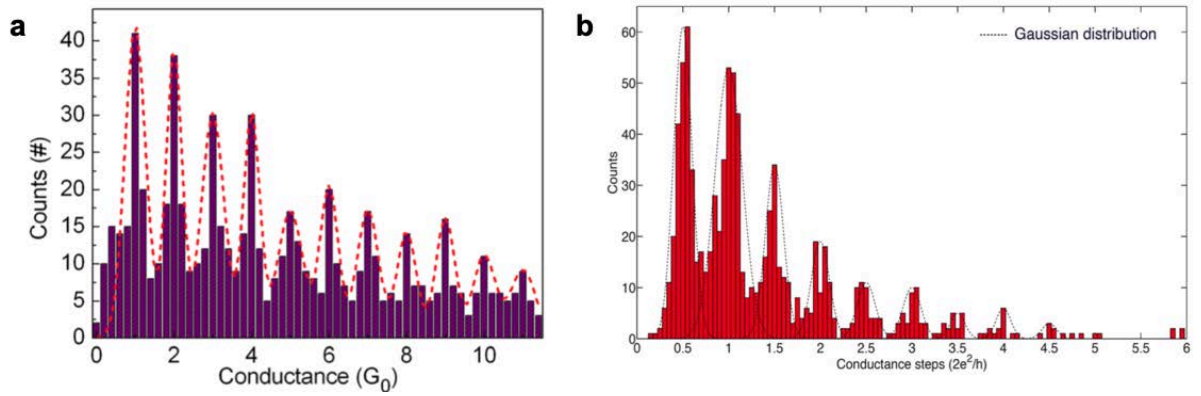


**Figure 4.** Statistical analysis of quantized conductance levels in memristive devices. **a** Histogram of conductance quantized levels by considering 662 conductance points in 22 different Ti/Ta<sub>2</sub>O<sub>5</sub>/Pt memristive devices observed under voltage pulse stimulation mode. The dashed line represents Gaussian fitting curve. Reproduced with permission.<sup>[30]</sup> Copyright 2014, AIP Publishing. **b** Histogram of conductance changes during ~1000 conductance steps recorded in voltage sweep operational mode in a SiO<sub>x</sub>-based memristive device. Peaks at half-integer multiples of  $G_0$  can be observed. The dashed lines represent Gaussian fitting curves. Reproduced under the terms of Creative Commons Attribution 3.0 License.<sup>[37]</sup> Copyright 2013, Nature Publishing Group.

Besides stochasticity and time variability, a source of uncertainty can be represented also by the presence of parasitic resistances that can alter the value of the quantum point contact resistance, as schematized in Figure 5. Here, the quantized resistance due to filament constriction  $R_c$  is in series with the filament bulk resistance  $R_f$  and the resistance associated to the metallic electrodes  $R_e$ , while electrons flowing in the insulating matrix outside the filament give rise to a parallel channel for electronic conduction associated to the parallel parasitic resistance  $R_i$ . Due to the metallic nature of the contact,  $R_e$  can be usually neglected since  $R_e \ll R_c$ . Also, the effect of the parallel resistance  $R_i$  can be negligible ( $R_i \gg R_c$ ) by properly design the

device geometry and by appropriate selection of the insulating materials. Instead, the bulk filament resistance  $R_f$  represents a source of uncertainty that cannot be neglected. As an example, the bulk filament resistance  $R_f$  was estimated to be  $\sim 800 \, \Omega$  in case of Ag/SiO<sub>2</sub>/Pt memristive devices.<sup>[46]</sup> However, since this value is strongly related to the filament morphology, this source of uncertainty needs to be evaluated on the specific memristive cell and operating conditions.

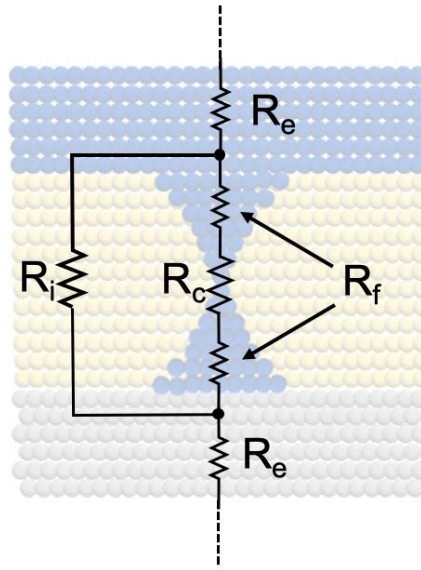


**Figure 5.** Equivalent electrical circuit of a memristive cell. Besides the quantized contact resistance  $R_c$ , the equivalent circuit is composed of the bulk filament resistance  $R_f$ , the resistance of the insulating active materials  $R_i$  and the resistance of the metallic electrodes  $R_e$ .

## Conclusions and perspectives

The redefinition of the SI opens the way for the development of new metrological experiments and devices able to correlate an observable physical quantity to fundamental physical constants. In this framework, memristive devices represent a promising platform for quantum electrical metrology exhibiting quantized conductance levels multiple of the fundamental quantum of conductance  $G_0 = 2e^2/h$ . As discussed in this work, working principles of memristive devices are based on nanoionic processes responsible for resistive switching behaviour underlying quantized conductance phenomena. Quantized conductance behaviour is related to electrically-

induced quantum point contacts realized by manipulating ions with consequent atomic rearrangement at the nanoscale. This means that ionic processes are coupled to the electronic ones, differently from conventional quantum-Hall devices where quantized conductance levels are determined only by purely electronic phenomena occurring in presence of an external magnetic field. As a direct consequence of coupling ionics with electronics in two-terminal memristive devices, it is possible to observe quantized conductance phenomena in air at room temperature and without applying any external magnetic field. In perspective, particularly promising results the scalability of the memristive device that was demonstrated down to the critical size of  $< 2 \text{ nm}^{[47]}$ , the high operational speed ( $< 1 \text{ ns}^{[48]}$ ) and the low power consumption for programming the internal conductance state ( $< \text{pJ}^{[49]}$ ). In addition, it is worth noticing that common materials for memristive devices such as transition metal oxides, perovskites and metal electrodes are compatible with CMOS technology not only in terms of materials and processing techniques but also in terms of electrical performances.<sup>[50,51]</sup> All these characteristics makes memristive devices particularly promising for on-chip integration of a standard of resistance. In the light of the new SI, this represents an important breakthrough for electrical metrology, allowing the realization of embedded self-calibrating systems and equipments with traceability to the fundamental physical quantities. Also, it is important to mention that a standard of resistance coupled with a voltage standard (realized for example by exploiting the Josephson effect) is a possible route for the practical realization of a current standard as indicated by the Bureau International des Poids et Mesures.<sup>[4]</sup> However, the main challenges for exploiting memristive devices for metrology are related to the intrinsic stochasticity of ionic processes underlying resistive switching effects that affect reproducibility and variability over time of quantized conductance levels. In order to overcome these issues, a deep understanding and control nanoionics processes underlying memristive behaviour is required. Moreover, one of the main challenges still remain to uncover the relationship between the involved materials and device functionalities. In this scenario, the development of memristive devices with

quantized conductance levels for the realization of a resistance standard necessarily imply an optimization of the involved materials and their interfaces as well as the operating conditions. All these challenges towards the realization of a resistance standard based on memristive devices have to be faced by taking into consideration the level of uncertainty required for each specific application.

Received: ((will be filled in by the editorial staff))

Revised: ((will be filled in by the editorial staff))

Published online: ((will be filled in by the editorial staff))

## References

- [1] J. Fischer, J. Ullrich, *Nat. Phys.* **2016**, *12*, 4.
- [2] E. Göbel, U. Siegner, *The New International System of Units (SI)*, Wiley, **2019**.
- [3] F. Piquemal, B. Jeckelmann, L. Callegaro, J. Hällström, T. J. B. M. Janssen, J. Melcher, G. Rietveld, U. Siegner, P. Wright, M. Zeier, *Metrologia* **2017**, *54*, R1.
- [4] BIPM Bureau International des Poids et Mesures, *The International System of Units (SI Brochure) [9th Edition]*, **2019**.
- [5] W. Poirier, S. Djordjevic, F. Schopfer, O. Thévenot, *Comptes Rendus Phys.* **2019**, *20*, 92.
- [6] K. von Klitzing, *Nat. Phys.* **2017**, *13*, 198.
- [7] K. V. Klitzing, G. Dorda, M. Pepper, *Phys. Rev. Lett.* **1980**, *45*, 494.
- [8] K. von Klitzing, *Rev. Mod. Phys.* **1986**, *58*, 519.
- [9] K. S. Novoselov, Z. Jiang, Y. Zhang, S. V. Morozov, H. L. Stormer, U. Zeitler, J. C. Maan, G. S. Boebinger, P. Kim, A. K. Geim, *Science (80-. )*. **2007**, *315*, 1379.
- [10] D. B. Strukov, G. S. Snider, D. R. Stewart, R. S. Williams, *Nature* **2008**, *453*, 80.
- [11] R. Waser, R. Dittmann, G. Staikov, K. Szot, *Adv. Mater.* **2009**, *21*, 2632.
- [12] R. Waser, M. Aono, *Nat. Mater.* **2007**, *6*, 833.
- [13] I. Valov, R. Waser, J. R. Jameson, M. N. Kozicki, *Nanotechnology* **2011**, *22*, 289502.
- [14] J. Joshua Yang, F. Miao, M. D. Pickett, D. A. A. Ohlberg, D. R. Stewart, C. N. Lau, R. S. Williams, *Nanotechnology* **2009**, *20*, 215201.
- [15] A. Sawa, *Mater. Today* **2008**, *11*, 28.
- [16] G. Milano, S. Porro, I. Valov, C. Ricciardi, *Adv. Electron. Mater.* **2019**, *5*, 1800909.
- [17] W.-P. Lin, S.-J. Liu, T. Gong, Q. Zhao, W. Huang, *Adv. Mater.* **2014**, *26*, 570.
- [18] Y. Li, S. Long, Y. Liu, C. Hu, J. Teng, Q. Liu, H. Lv, J. Suñé, M. Liu, *Nanoscale Res. Lett.* **2015**, *10*, 420.
- [19] W. Xue, S. Gao, J. Shang, X. Yi, G. Liu, R. Li, *Adv. Electron. Mater.* **2019**, *5*, 1800854.
- [20] H. van Houten, C. Beenakker, *Phys. Today* **1996**, *49*, 22.
- [21] N. Agraït, *Phys. Rep.* **2003**, *377*, 81.
- [22] E. Miranda, D. Jimenez, J. Sune, *IEEE Electron Device Lett.* **2012**, *33*, 1474.
- [23] X. Lian, X. Cartoixa, E. Miranda, L. Perniola, R. Rurali, S. Long, M. Liu, J. Suñé, *J. Appl. Phys.* **2014**, *115*, 244507.
- [24] J. Hajto, A. E. Owen, S. M. Gage, A. J. Snell, P. G. LeComber, M. J. Rose, *Phys. Rev. Lett.* **1991**, *66*, 1918.
- [25] E. Yun, M. F. Becker, R. M. Walser, *Appl. Phys. Lett.* **1993**, *63*, 2493.



- [26] K. Terabe, T. Hasegawa, T. Nakayama, M. Aono, *Nature* **2005**, 433, 47.
- [27] J. Zhao, Z. Zhou, Y. Zhang, J. Wang, L. Zhang, X. Li, M. Zhao, H. Wang, Y. Pei, Q. Zhao, Z. Xiao, K. Wang, C. Qin, G. Wang, H. Li, B. Ding, F. Yan, K. Wang, D. Ren, B. Liu, X. Yan, *J. Mater. Chem. C* **2019**, 7, 1298.
- [28] T. Tsuruoka, T. Hasegawa, K. Terabe, M. Aono, *Nanotechnology* **2012**, 23, 435705.
- [29] L. Jiang, L. Xu, J. W. Chen, P. Yan, K. H. Xue, H. J. Sun, X. S. Miao, *Appl. Phys. Lett.* **2016**, 109, 153506.
- [30] C. Chen, S. Gao, F. Zeng, G. Y. Wang, S. Z. Li, C. Song, F. Pan, *Appl. Phys. Lett.* **2013**, 103, 043510.
- [31] F. G. Aga, J. Woo, J. Song, J. Park, S. Lim, C. Sung, H. Hwang, *Nanotechnology* **2017**, 28, 115707.
- [32] C. Hu, M. D. McDaniel, A. Posadas, A. A. Demkov, J. G. Ekerdt, E. T. Yu, *Nano Lett.* **2014**, 14, 4360.
- [33] E. Miranda, S. Kano, C. Dou, K. Kakushima, J. Suñé, H. Iwai, *Appl. Phys. Lett.* **2012**, 101, 012910.
- [34] X. Zhao, H. Xu, Z. Wang, L. Zhang, J. Ma, Y. Liu, *Carbon N. Y.* **2015**, 91, 38.
- [35] X. Zhu, W. Su, Y. Liu, B. Hu, L. Pan, W. Lu, J. Zhang, R.-W. Li, *Adv. Mater.* **2012**, 24, 3941.
- [36] S. Tappertzhofen, I. Valov, R. Waser, *Nanotechnology* **2012**, 23, 145703.
- [37] A. Mehonic, A. Vrajitoarea, S. Cueff, S. Hudziak, H. Howe, C. Labbé, R. Rizk, M. Pepper, A. J. Kenyon, *Sci. Rep.* **2013**, 3, 2708.
- [38] W. Banerjee, H. Hwang, *Adv. Electron. Mater.* **2019**, 1900744, 1900744.
- [39] S. U. Sharath, S. Vogel, L. Molina-Luna, E. Hildebrandt, C. Wenger, J. Kurian, M. Duerrschnabel, T. Niermann, G. Niu, P. Calka, M. Lehmann, H.-J. Kleebe, T. Schroeder, L. Alff, *Adv. Funct. Mater.* **2017**, 27, 1700432.
- [40] S. Long, X. Lian, C. Cagli, X. Cartoixa, R. Rurali, E. Miranda, D. Jiménez, L. Perniola, M. Liu, J. Suñé, *Appl. Phys. Lett.* **2013**, 102, 183505.
- [41] A. Younis, D. Chu, S. Li, *J. Mater. Chem. C* **2014**, 2, 10291.
- [42] K. Krishnan, M. Muruganathan, T. Tsuruoka, H. Mizuta, M. Aono, *Adv. Funct. Mater.* **2017**, 27, 1605104.
- [43] I. Valov, E. Linn, S. Tappertzhofen, S. Schmelzer, J. van den Hurk, F. Lentz, R. Waser, *Nat. Commun.* **2013**, 4, 1771.
- [44] G. Milano, M. Luebben, Z. Ma, R. Dunin-Borkowski, L. Boarino, C. F. Pirri, R. Waser, C. Ricciardi, I. Valov, *Nat. Commun.* **2018**, 9, 5151.
- [45] W. Wang, M. Wang, E. Ambrosi, A. Bricalli, M. Laudato, Z. Sun, X. Chen, D. Ielmini, *Nat. Commun.* **2019**, 10, 81.
- [46] S. Tappertzhofen, E. Linn, S. Menzel, A. J. Kenyon, R. Waser, I. Valov, *IEEE Trans. Nanotechnol.* **2015**, 14, 505.
- [47] S. Pi, C. Li, H. Jiang, W. Xia, H. Xin, J. J. Yang, Q. Xia, *Nat. Nanotechnol.* **2019**, 14, 35.
- [48] B. J. Choi, A. C. Torrezan, J. P. Strachan, P. G. Kotula, A. J. Lohn, M. J. Marinella, Z. Li, R. S. Williams, J. J. Yang, *Adv. Funct. Mater.* **2016**, 26, 5290.
- [49] F. Hui, E. Grustan-Gutierrez, S. Long, Q. Liu, A. K. Ott, A. C. Ferrari, M. Lanza, *Adv. Electron. Mater.* **2017**, 3, 1600195.
- [50] S. H. Jo, W. Lu, *Nano Lett.* **2008**, 8, 392.
- [51] F. Cai, J. M. Correll, S. H. Lee, Y. Lim, V. Bothra, Z. Zhang, M. P. Flynn, W. D. Lu, *Nat. Electron.* **2019**, 2, 290.

Memristive devices exhibiting quantum conductance levels are proposed as quantum metrology devices in the light of the redefinition of the International System of Units (SI). Due to their high scalability, compatibility with CMOS technology, memristive devices working in air at room temperature represent promising platforms for on-chip embedding of a resistance standard for realizing self-calibrating systems with zero-chain traceability.

## Quantum metrology

**Gianluca Milano\*, Federico Ferrarese Lupi, Matteo Fretto, Carlo Ricciardi, Natascia De Leo, Luca Boarino**

### Memristive devices for quantum metrology

